Effect of annealing on the temperature-dependent dielectric properties of LaAlO3 at terahertz frequencies

Xingquan Zou, Mi He, Daniel Springer, Dongwook Lee, Saritha K. Nair et al.

Citation: AIP Advances **2**, 012120 (2012); doi: 10.1063/1.3679725
View online: http://dx.doi.org/10.1063/1.3679725
View Table of Contents: http://aipadvances.aip.org/resource/1/AAIDBI/v2/i1
Published by the American Institute of Physics.

Effect of annealing on the temperature-dependent dielectric properties of $LaAlO_3$ at terahertz frequencies

Xingquan Zou,[1] Mi He,[1] Daniel Springer,[1] Dongwook Lee,[1] Saritha K. Nair,[1] Siew Ann Cheong,[1] Tom Wu,[1] C. Panagopoulos,[1] D. Talbayev,[2] and Elbert E. M. Chia[1,a]

[1]*Division of Physics and Applied Physics, School of Physical and Mathematical Sciences, Nanyang Technological University, Singapore 637371, Singapore*

[2]*Department of Physics and Engineering Physics, 2001 Percival Stern Hall, 6400 Freret street, New Orleans, Louisiana 70118, USA*

(Received 2 November 2011; accepted 2 January 2012; published online 13 January 2012)

We present THz conductivity of $LaAlO_3$ (LAO) as a function of temperature and annealing, using terahertz time-domain spectroscopy (THz-TDS). We observed that, after annealing, spectral weight redistribution occurs, such that the real conductivity $\sigma_1(\omega)$ changed from a featureless and almost frequency-independent spectrum, into one where peaks occur near the phonon frequencies. These phonon frequencies increase with increasing temperature. We attribute the appearance of these absorption peaks to the diffusion and relocation of oxygen vacancies. The dielectric functions of annealed LAO are well fitted with the Drude-Lorentz model. [doi:10.1063/1.3679725]

Lanthanum aluminate ($LaAlO_3$, LAO) is a rhombohedrally-distorted perovskite commonly used as a substrate for high-temperature superconductors and functional thin films.[1] The cubic-to-rhombohedral transition in LAO is attributed to the rotation or tilt of the oxygen octahedra (AlO_6) along the (111) cubic unit cell direction. This rotation angle serves as an order parameter across the phase transition ($T_c \approx 850$ K).[2] In order to understand the structural and optical properties of LAO, many experimental and theoretical studies have been done, for example, neutron diffraction, Raman and infrared spectra, etc.[3–6] The microwave (4 GHz - 12 GHz) absorption of single crystal LAO at different temperatures (4 K - 300 K) have been investigated by Zuccaro *et al.*.[7] They pointed out that the dielectric loss in LAO is due to microwave absorption by phonons and relaxation of dipoles brought about by defects in the crystal. Room-temperature absorption spectra were also studied at terahertz (THz) frequencies which contain information of large molecule and intermolecular vibrations.[8,9]

In addition, LAO is one of the most commonly used substrates in the growth of complex functional thin films such as high-temperature superconductors, multiferroics and manganites. In such strongly correlated electron systems, due to the presence of many competing degrees of freedom (e.g. orbital, lattice, electronic, spin), and the absence of a dominant energy scale, low-energy dynamics, particularly at THz (or far-infrared) frequencies, frequently reveal the interplay among these different degrees of freedom.[10] In THz studies, a reliable extraction of the temperature-dependent complex conductivity (or equivalently, refractive index) of the thin film depends critically on the complex refractive index of the underlying LAO substrate, at every temperature. Moreover, since thin-film growth invariably involves annealing, the effects of annealing on the optical properties of LAO must also be taken into account. Furthermore, it is well known that domains are present in LAO substrates, but their effect on the optical properties of LAO is not known. As far as we know, no systematic temperature or annealing-dependent studies have been carried out on LAO

[a]Electronic mail: elbertchia@ntu.edu.sg

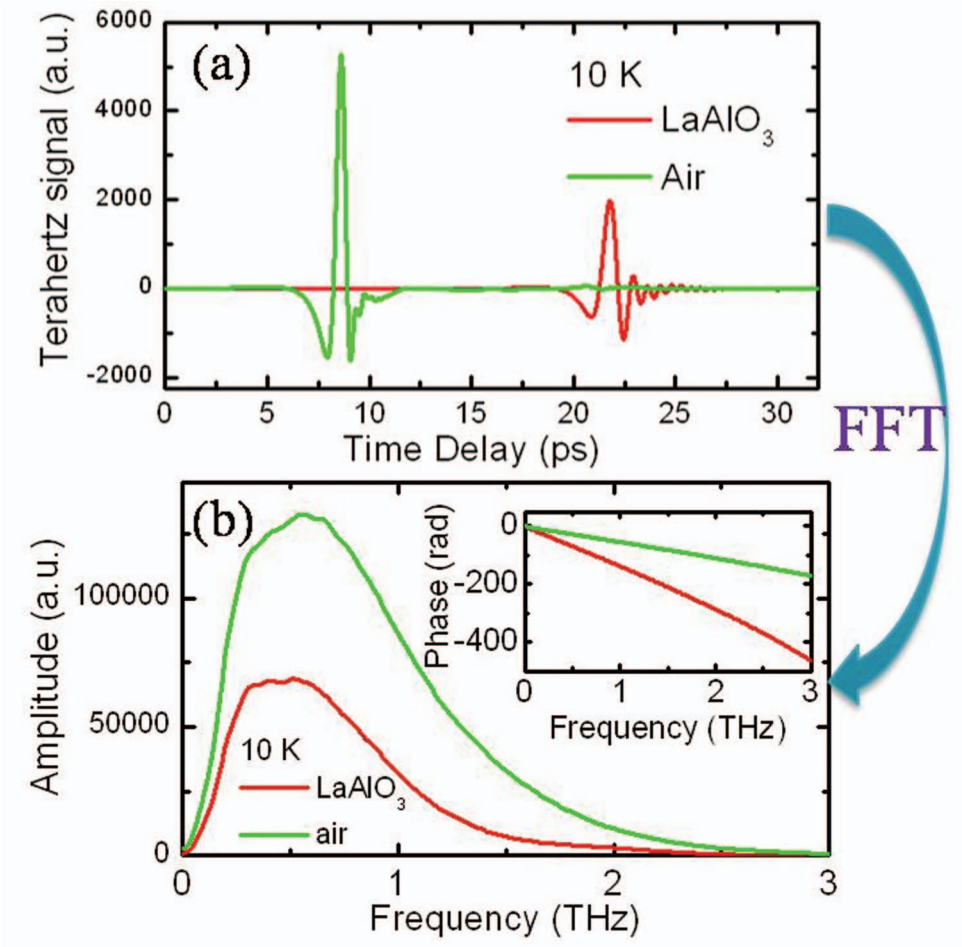

FIG. 1. (Color online) (a) Time-domain terahertz signal from sample LAO (without annealing) and air reference at 10 K. (b) Amplitude and phase spectra in the frequency domain from the FFT of (a).

at THz frequencies. Our work fills this gap in knowledge, enabling future researchers to use the temperature-dependent refractive index of LAO to characterize their thin films more accurately. Here we report the temperature-dependent (10 K - 300 K) dielectric response of LAO by terahertz time-domain spectroscopy (THz-TDS) from 0.2 THz − 3 THz. After annealing, strong absorption peaks appear in $k(\omega)$, with peak positions shifting to higher frequencies with increasing temperature.

Our investigated samples are single crystals of (100) LAO: a $10\times10\times1$ mm^3 piece from CrysTec GmbH (Berlin, Germany), and a $10\times10\times0.5$ mm^3 piece from SWI (Hsinchu, Taiwan). Since both samples give the similar results, we only show data from the CrysTec sample. The dielectric response of LAO was measured by a commercial THz-TDS system (TeraView Spectra 3000). From THz-TDS, we can directly obtain material dielectric parameters[11–14] like complex refractive index $\tilde{n}(\omega) = n(\omega) + ik(\omega)$, optical conductivity $\tilde{\sigma}(\omega) = \sigma_1(\omega) + i\sigma_2(\omega)$ and dielectric function $\tilde{\varepsilon}(\omega) = \varepsilon_1(\omega) + i\varepsilon_2(\omega)$.

The time-domain electric fields of a THz pulse transmitted through the LAO sample ($\tilde{E}_s(t)$), as well as through air reference ($\tilde{E}_r(t)$) are shown in Fig. 1(a). The THz wave form was attenuated and delayed after passing through LAO sample. Fast Fourier transform yields the amplitude and phase at different spectra components of the THz electromagnetic wave, as shown in Fig. 1(b). Without invoking Kramers-Kronig relations, the complex refractive index $\tilde{n}(\omega)$ can be obtained by numerically solving the equation:[15]

$$\tilde{T}(\omega) = \frac{\tilde{E}_s(\omega)}{\tilde{E}_r(\omega)} = \frac{4\tilde{n}(\omega)}{(1+\tilde{n}(\omega))^2}\exp[i\omega d(\tilde{n}(\omega)-1)/c], \quad (1)$$

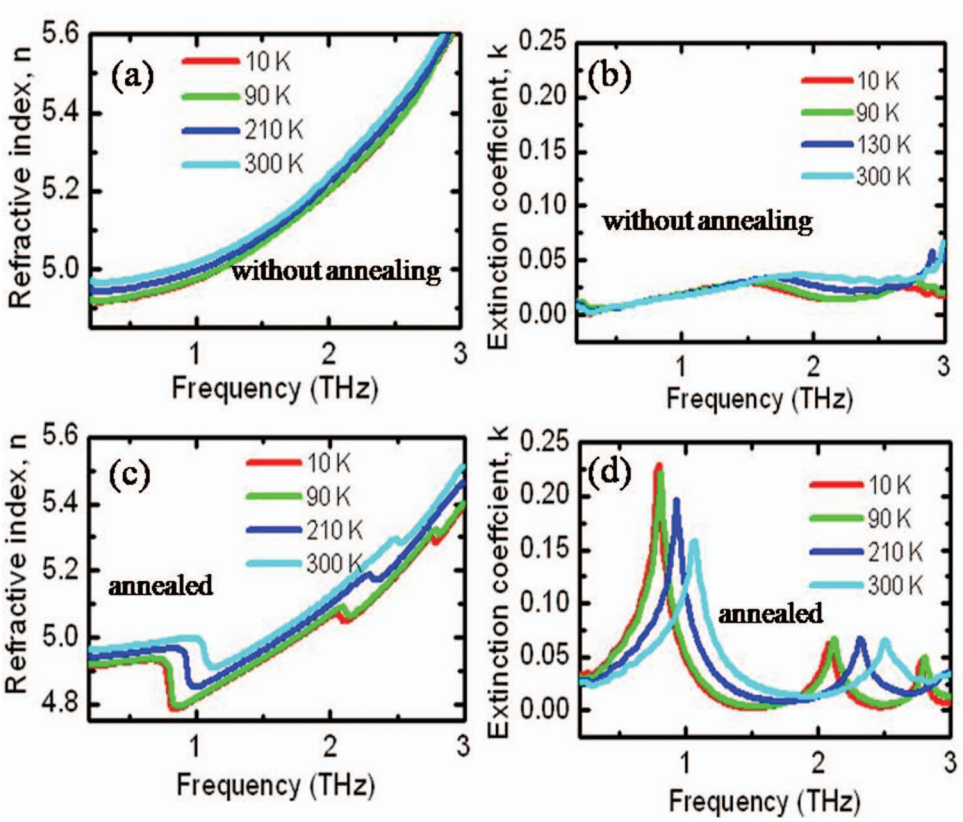

FIG. 2. (Color online) Extracted refractive index n and extinction coefficient k of LAO before and after annealing treatment at different temperatures. Before annealing (a), (b) and after annealing (c), (d).

where $\tilde{T}(\omega)$, $\tilde{n}(\omega)$, d, c are complex transmittance, LAO complex refractive index, sample thickness and speed of light (in vacuum) respectively.

The refractive index $n(\omega)$ and extinction coefficient $k(\omega)$ of LAO (without annealing) at different temperatures are shown in Figs. 2(a) and 2(b). $n(\omega)$ is temperature-dependent and increases monotonically with frequency. The values of $k(\omega)$ are very small, and no obvious absorption peaks appeared in our experimental frequency range. The extracted $n(\omega)$ and $k(\omega)$ are consistent with other reports[4,9] at 300 K. Next, after the LAO is annealed under the condition of 1273 K in vacuum for 3 hours, and THz-TDS data were taken at the same orientation as before, the extracted $n(\omega)$ exhibits jumps at certain frequencies (Fig. 2(c)), where it suddenly drops, then recovers slowly with frequency. Also, several absorption peaks appear in $k(\omega)$ (Fig. 2(d)). These absorption peaks are temperature-dependent — shifting to the higher frequency with increasing temperature.

We attribute the appearance of absorption peaks in $k(\omega)$ after annealing to a relocation of oxygen vacancies in the LAO crystal. Before annealing, below 730 K, the immobile oxygen vacancies form clusters and effectively pin the domain walls.[3] During the annealing of LAO at 1273 K, the self-diffusion coefficient of these oxygen vacancies increase significantly at high temperature.[8] As the oxygen vacancies diffuse and relocate throughout the crystal, the effect of pinning will be reduced, resulting in the domain walls becoming more mobile, until they disappear.

The real part of optical conductivity $\sigma_1(\omega)$ can be obtained from the relationship $\sigma_1(\omega) = 2n(\omega)k(\omega)\omega\varepsilon_0$. Figure 3 shows the spectrum of $\sigma_1(\omega)$ before and after annealing, at different temperatures. Before annealing, in the "as-is" sample, $\sigma_1(\omega)$ increases slightly with frequency, and does not show any sharp features. Upon annealing, however, temperature-dependent peaks develop in $\sigma_1(\omega)$. Comparing the $\sigma_1(\omega)$ before and after annealing in Fig. 3, we noticed that, after annealing, $\sigma_1(\omega)$ exhibits peaks only at some particular frequencies, and is almost zero away from these frequencies. This indicates the spectral weight is redistributed and transferred towards these frequencies

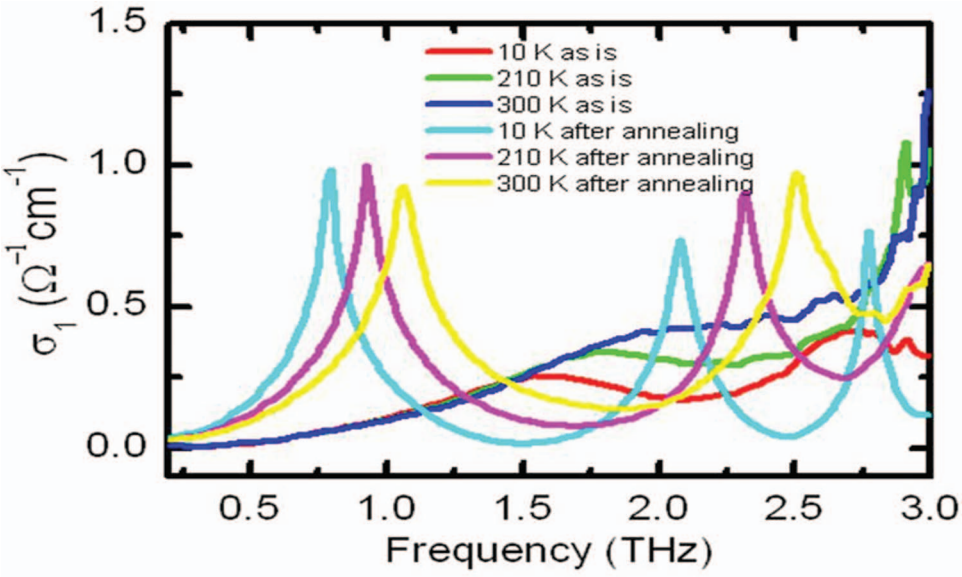

FIG. 3. (Color online) Real part conductivity of LAO before and after annealing at various temperatures.

after annealing. Annealing above the transition temperature T_c will usually relax the thermal strains and redistribute the oxygen defects, causing twin walls to appear elsewhere and in different orientations when the crystal is again cooled to below T_c.[16]

In order to probe the origin of these temperature-dependent absorption peaks, we compute the complex dielectric function of annealed LAO from $n(\omega)$ and $k(\omega)$ by the relations: $\varepsilon_1(\omega) = n(\omega)^2 - k(\omega)^2$ and $\varepsilon_2(\omega) = 2n(\omega)k(\omega)$. The real and imaginary parts of dielectric function are simultaneously fitted with the Drude-Lorentz model.[17,18] In this model, frequency-dependent dielectric function can be described by summing over various oscillators and a residual Drude contribution:

$$\tilde{\varepsilon}(\omega) = \varepsilon_\infty - \frac{\omega_p^2}{\omega^2 + i\Gamma_0\omega} + \sum_k \frac{A_k\omega_k^2}{\omega_k^2 - \omega^2 - i\Gamma_k\omega}. \quad (2)$$

The first term ε_∞ is the high-frequency dielectric constant $\varepsilon_\infty = 4.82$;[6,19] the second term is the Drude term, which describes the response of the unbound (free) charge carriers; ω_p and Γ_0 are the plasma frequency and scattering rate of free electrons, respectively. The last term describes a collection of Lorentz oscillators, where A_k, ω_k, Γ_k are the oscillator strength, oscillator resonance frequency and oscillator damping constant (spectral width) of the k^{th} oscillator, respectively.

To obtain a good fit, we used four Lorentz oscillators. Fig. 4(a) shows the real and imaginary parts of $\tilde{\varepsilon}(\omega)$, and the corresponding Drude-Lorentz model fitting, where, for the sake of clarity, only the 10 K data and fitting are presented. Generally, THz absorption is attributed to the interactions of THz field with the fundamental lattice vibrations in the crystal. The optical modes of Brillouin zone center associated with the first-order dipole moment give rise to intrinsic absorption due to lattice vibrations. Among the four resonances, the strongest absorption peak ω_1 is located at ~6 THz with a temperature-independent peak position. This strong (A_1~18) 6 THz peak corresponds to the main infrared (IR) triplet mode at 167 cm^{-1} in the undistorted perovskite, which transforms into the 168 cm^{-1} A_{2u} IR singlet and 179 cm^{-1} E_u IR doublet upon undergoing rhombohedral distortion.[20] The other three resonances ($\omega_2 \sim 1.0$ THz, $\omega_3 \sim 2.5$ THz, $\omega_4 \sim 3.6$ THz at 300 K) are much weaker than ω_1, with temperature-dependent peak positions — shifting to higher frequency with increasing temperature, as shown in Fig. 4(b). It has been confirmed experimentally and theoretically that Raman modes in LAO[5,6] appear at ~1 THz and ~3.7 THz. The observation of the 1 THz (ω_2) and 3.6 THz (ω_4) modes in our data showed that, upon annealing, these Raman modes have acquired IR character as well. This is not surprising, as lattice distortion induced at high temperatures (~773 K)

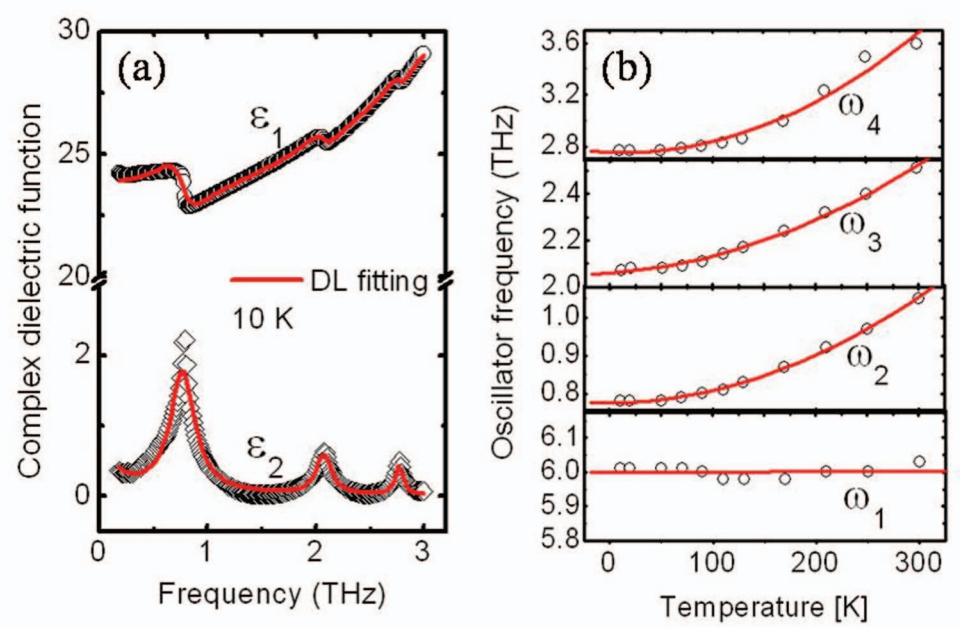

FIG. 4. (Color online) (a) Real and imaginary parts of dielectric function of LAO and the Drude-Lorentz model fitting. (b) Oscillator frequencies evolve with temperature, red lines are linear fitting for ω_1 and quadratic fitting for ω_2, ω_3 and ω_4.

may have caused an asymmetry in the lattice structure that results in the appearance of absorption peaks at these previously Raman-active frequencies.[8] Our temperature-dependent ω_3 has not been reported before — it possibly originates from multiple phonon processes.[14]

We now discuss the phonon stiffening with increasing temperature. Normally, the frequency change of every lattice mode is related to the rate of change in volume V of the crystal as: $\frac{\Delta f}{f} = -\gamma \frac{\Delta V}{V}$, where γ is an average Grüneisen constant. In most materials, $\gamma > 0$, so phonon soften upon thermal expansion. This thermal expansion and associated shift of phonon frequencies stem from the anharmonic components in interatomic potentials, which are responsible for the scattering between harmonic phonon quasiparticles. However, Delaire *et al.*[21] found that the phonon energies in metallic vanadium effectively stiffen with increasing temperature, compensating for the effect of thermal expansion. They attribute this to the coupling between phonons and the electron bandstructure — an adiabatic electron-phonon interaction. For LAO crystal, the AlO_6 structural unit (AlO_6) can undergo dynamics at low energies by rotating as a rigid unit. These rigid unit modes of AlO_6 can break the symmetry of a structure of packed octahedra, and can be responsible for displacive phase transformations in minerals. Also, some oxygen atoms at the corners of AlO_6 are not shared by other octahedra, hence they will have more freedom to be involved in the reorientations.[22] These features may be responsible for the phonon stiffening with increasing temperature in the annealed LAO crystal. The low energy vibrational modes in ZrW_2O_8 and $HfMo_2O_8$, with similar local structure as LAO, also show a stiffening with increasing temperature.[22] To fully elucidate the phonon frequencies stiffening with increasing temperature, more theoretical calculation is needed.

In conclusion, temperature-dependent THz dielectric response of as-is and annealed LAO have been studied using THz-TDS from 0.2 THz - 3 THz. Annealing greatly affects its optical properties. The appearance of the absorption peaks in $k(\omega)$ upon annealing is attributed to the diffusion and relocation of oxygen vacancies — these disordered oxygen vacancies reduce the pinning effects on the domain walls in the LAO crystal. The change of $\sigma_1(\omega)$ from featureless, to peaks occurring at certain frequencies, is attributed to spectral weight transfer.

The authors acknowledge support from Singapore Ministry of Education Academic Research Fund Tier 2 (Grant No. ARC 23/08), as well as the National Research Foundation Competitive

Research Programme (Grant No. NRF-CRP4-2008-04). We thank Venky Venkatesan and Sankar Dhar for useful discussions.

[1] R. J. Zeches, M. D. Rossell, J. X. Zhang, A. J. Hatt, Q. He, C. H. Yang, A. Kumar, C. H. Wang, A. Melville, C. Adamo, G. Sheng, Y. H. Chu, J. F. Ihlefeld, R. Erni, C. Ederer, V. Gopalan, L. Q. Chen, D. G. Schlom, N. A. Spaldin, L. W. Martin, and R. Ramesh, Science **326**, 977 (2009).
[2] S. A. Hayward, S. A. T. Redfern, and E. K. H. Salje, J. Phys.: Condens. Matter **14**, 10131 (2002).
[3] S. A. Hayward, F. D. Morrison, S. A. T. Redfern, E. K. H. Salje, J. F. Scott, K. S. Knight, S. Tarantino, A. M. Glazer, V. Shuvaeva, P. Daniel, M. Zhang, and M. A. Carpenter, Phys. Rev. B **72**, 054110 (2005).
[4] Z. M. Zhang, B. I. Choi, M. I. Flik, and A. C. Anderson, J. Opt. Soc. Am. B **11**, 2252 (1994).
[5] V. G. Sathe and A. Dubey, J. Phys.: Condens. Matter **19**, 382201 (2007).
[6] P. Delugas, V. Fiorentini, and A. Filippetti, Phys. Rev. B **71**(13), 134302 (2005).
[7] C. Zuccaro, M. Winter, N. Klein, and K. Urban, J. Appl. Phys. **82**, 5695 (1997).
[8] K. Nomura, S. Okami, X. J. Xie, M. Mizuno, K. Fukunaga, and Y. Ohki, Jpn. J. Appl. Phys. **50**, 021502 (2011).
[9] D. Grischkowsky and S. Keiding, Appl. Phys. Lett. **57**, 1055 (1990).
[10] R. D. Averitt and A. J. Taylor, J. Phys.: Condens. Matter **14**, R1357 (2002).
[11] J. Shan, F. Wang, E. Knoesel, M. Bonn, and T. F. Heinz, Phys. Rev. Lett. **90**, 247401 (2003).
[12] K. R. Mavani, M. Nagai, D. S. Rana, H. Yada, I. Kawayama, M. Tonouchi, and K. Tanaka, Appl. Phys. Lett. **93**, 231908 (2008).
[13] J. B. Baxter and C. A. Schmuttenmaer, Phys. Rev. B **80**, 235205 (2009).
[14] J. G. Han, B. K. Woo, W. Chen, M. Sang, X. C. Lu, and W. L. Zhang, J. Phys. Chem. C **112**, 17512 (2008).
[15] L. Duvillaret, F. Garet, and J. L. Coutaz, IEEE J. Sel. Top. Quantum Electron. **2**, 739 (1996).
[16] S. Bueble, K. Knorr, E. Brecht, and W. W. Schmahl, Surf. Sci. **400**, 345 (1998).
[17] A. B. Kuzmenko, Rev. Sci. Instrum. **76**, 083108 (2005).
[18] D. Talbayev, A. D. LaForge, S. A. Trugman, N. Hur, A. J. Taylor, R. D. Averitt, and D. N. Basov, Phys. Rev. Lett. **101**, 247601 (2008).
[19] R. Vali, Comput. Mater. Sci. **44**, 779 (2008).
[20] Pietro Delugas, Vincenzo Fiorentini, and Alessio Filippetti, Phys. Rev. B **71**, 134302 (2005).
[21] O. Delaire, M. Kresch, J. A. Munoz, M. S. Lucas, J. Y. Y. Lin, and B. Fultz, Phys. Rev. B **77**, 214112 (2008).
[22] B. Fultz, Prog. Mater Sci. **55**, 247 (2010).